Development of a Functionalizable External β-Turn Mimic Based on a *cis*-Fused 1,7-Naphthyridine Scaffold

Frederik J. R. Rombouts,[a] Wim M. De Borggraeve,[a] David Delaere,[b] Matheus Froeyen,[c] Suzanne M. Toppet,[a] Frans Compernolle,[a] and Georges J. Hoornaert*[a]

Keywords: Bioorganic chemistry / Conformation analysis / Cycloaddition / Naphthyridine / Peptidomimetics

An intramolecular Diels–Alder strategy using 2(1*H*)-pyrazinones was applied to generate a substituted perhydro-1,7-naphthyridine ring system that served as a scaffold to construct the type VI β-turn mimic **2**, featuring a *cis*-amide linkage between the central *i*+1 and *i*+2 residues. The synthesis permits mimicking of the amino acid side chains of the central dipeptide, a unique feature for external-turn mimics. Modeling studies indicated that the *cis*-fused bicyclic system adopts a conformation suitable for induction of a β-turn when the angular position 8a bears a non-H substituent. Extensive NMR analysis of an 8a-methyl derivative **25** confirmed its β-turn-inducing properties in various solvents, including water.

Introduction

With helices and sheets, turns comprise the third major motif of peptide and protein secondary structure. A turn can be defined as the site at which a peptide changes its overall direction. Different types of turns have been described, including δ-, γ-, β-, α-, and π-turns corresponding to loops involving two to six residues, respectively.[1] Of these, the most common naturally occurring type is the β-turn, which reverses direction over four residues, often with a hydrogen bond between the carbonyl group of residue *i* and the NH moiety of residue *i*+3. The prevalence of β-turns in peptides and on protein surfaces suggests that they play essential roles in molecular recognition events in biological systems, such as receptor−ligand, enzyme−substrate, and antigen−antibody interactions. This has raised the challenge of the development of functionalizable β-turn mimics[2] to study these interactions or to enhance in vivo absorption and the metabolic stability of peptide probes.[3] Moreover, the incorporation of rigid β-turn analogues might render peptides more active by limiting solution conformations, thus lowering the entropy cost for binding and enhancing selectivity by preclusion of conformers that give rise to undesired bioactivity. In a previous communication[4] we reported the synthesis of the potential β-turn mimic **1** (Figure 1), which meets the criteria of functionalizability and rigidity. In a next phase of this investigation, we wanted to impose additional conformational restrictions into **1** in order further to rigidify its presumed β-turn-inducing structure. We thus envisioned the incorporation of the acetamide nitrogen atom in a six-membered ring, which should be *cis*-annelated to the piperidinone core in order to retain the spatial proximity to the carboxamide, as shown in structure **2**.

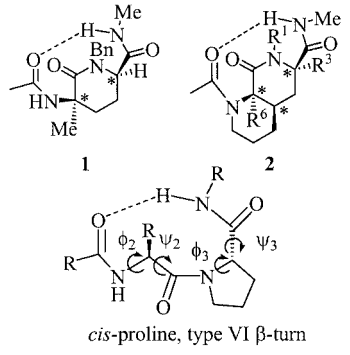

Figure 1. Type VI β-turn mimics **1** and **2** and the natural β-turn

Compounds **1** and **2** can be viewed as rigidified mimics of *cis*-amide turns such as the type VI β-turn, which has *cis*-proline at the *i*+2 position of a tetrapeptide entity. The type VI β-turn has been implicated in the bioactive conformations of several peptides.[5] Notably, *cis*-amide models

[a] Laboratorium voor Organische Synthese, K. U. Leuven, Celestijnenlaan 200F, 3001 Leuven, Belgium
Fax: (internat.) + 32-16/327990
E-mail: losh@chem.kuleuven.ac.be
[b] Groep Kwantumchemie, K. U. Leuven, Celestijnenlaan 200F, 3001 Leuven, Belgium
Fax: (internat.) + 32-16/327393
E-mail: David.Delaere@chem.kuleuven.ac.be
[c] Laboratorium voor Medicinale chemie, K. U. Leuven, Minderbroedersstraat 10, 3000 Leuven, Belgium
Fax: (internat.) + 32-16/337379
E-mail: Mathy.Froeyen@rega.kuleuven.ac.be
Supporting information for this article is available on the WWW under http://www.eurjoc.org or from the author.

  DOI: 10.1002/ejoc.200200652

might also serve as mimics of *cis*-amide moieties other than *cis*-proline, which, according to X-ray data, may occur more frequently than previously thought.[6] In our current approach, application of the 1,7-naphthyridine scaffold **2** for mimicking *cis*-amide β-turns is based on the following criteria:

(a) The *cis*-amide linkage between the central residues; this is constrained in a rigid bicyclic lactam system representing the $i+1$ and $i+2$ residues of the tetrapeptide.

(b) The spatial proximity of the residues attached to the N- and C-termini of the central dipeptide is enabled by the *cis* disposition of the N1 atom and the carboxamide group.

(c) The similarity of the bicyclic lactam structure **2** with that of other successful mimics of the type VI β-turn:[7] the latter mimics were also based on a lactam structure but they lacked the capacity to mimic various amino acid side chains, in contrast to the broad functionalization enabled by the variable R^3 and R^6 substituents in the general structure **2**.

Results and Discussion

In the following sections we first describe our synthetic approach to the 8a-H and 8a-substituted target molecules **2**. Next, we examine the conformational behavior of **2**, by use both of molecular modeling and of detailed NMR analysis. Finally the β-turn-inducing potential of 8a-substituted molecules is evaluated.

Synthesis

To construct the 1,7-naphthyridine scaffold we applied our recently reported intramolecular Diels–Alder reaction strategy using *N*-pentenyl-substituted 2(1*H*)-pyrazinones (Scheme 1; R^3 = Ph, R^6 = H).[8] Cycloaddition to form a bridged imidoyl chloride intermediate, followed by hydrolysis, provides stable tricyclic compounds exhibiting both a distorted tertiary amide and a nonstrained secondary amide function. The nonplanar tertiary amide can in turn be subjected to selective methanolysis to generate *cis*-fused bicyclic ring systems of type **2**. In a first approach we decided to use the already reported substitution pattern (R^3 = Ph, R^6 = H), but this did not provide the desired β-turn-inducing properties. According to modeling studies, an appropriate conformation should be imposed on the *cis*-fused bicyclic system through the introduction of a substituent R^6 = alkyl.

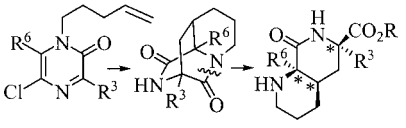

Scheme 1

Synthesis of 11

N-(*p*-Methoxybenzyl)pyrazinone **4** was generated by cyclization of 2-[*N*-(4-methoxybenzyl)amino]acetonitrile (HCl salt) **3** with oxalyl chloride (Scheme 2).[9] Subsequent Stille coupling, with tetraphenyltin and $[Pd(PPh_3)_4]$ as a catalyst, provided the corresponding 3-phenyl derivative **5**,[10] which was *N*-debenzylated by heating with trifluoroacetic acid to produce pyrazinone **6**. This was converted into the desired *N*-alkenylated pyrazinone **7** by heating with 5-bromo-1-pentene and Cs_2CO_3 in dioxane. Intramolecular cycloaddition of pyrazinone **7** and subsequent conversion of the resulting adduct **8** into bis(lactam) **9** were accomplished by heating **7** in bromobenzene at reflux temperature, followed by hydrolysis of the imidoyl chloride intermediate in water-saturated ethyl acetate. The strained tricyclic bis(lactam) **9** was converted into *cis*-fused 1,7-naphthyridine **10** by selective acid methanolysis of the tertiary amide group, effected by heating with 2.5 equiv. of methanesulfonic acid in boiling methanol. In the two final steps, amino ester **10** was transformed into target diamide **11** by *N*-acetylation of the free amino group, followed by aminolysis of the ester function by treatment with methylamine.

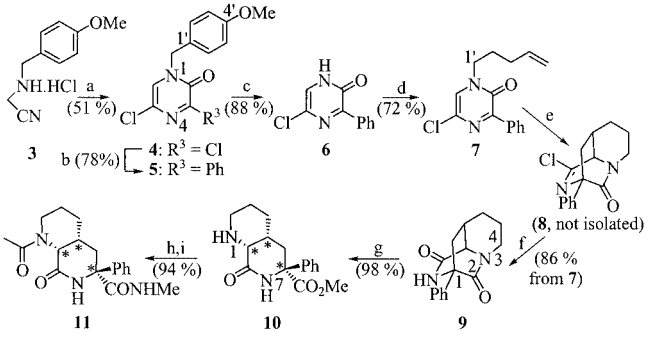

Scheme 2. a) $(COCl)_2$, $Et_3N{\cdot}HCl$, PhCl, room temp., 2 d; b) $SnPh_4$, $[Pd(PPh_3)_4]$, toluene, 120 °C, 7 d; c) CF_3CO_2H, reflux, 5 h; d) $Br(CH_2)_3CH{=}CH_2$, Cs_2CO_3, dioxane, 50 °C, 7 d; e) PhBr, reflux, overnight; f) EtOAc satd. with H_2O, room temp., overnight; g) MeOH, 2.5 equiv. CH_3SO_3H, reflux, overnight; h) Ac_2O, 40 °C, 1 h; i) 33 wt% CH_3NH_2/EtOH, room temp., overnight

Synthesis of 25

The sequence described above, used for the preparation of **11**, suffers from a very critical *N*-alkenylation step, in which cesium carbonate is used for selective *N*-alkenylation of pyrazinone **6** (Scheme 2, step d). Indeed, all methods other than the use of cesium carbonate tried out for this crucial step were found to give mainly *O*-alkylation. To investigate the tolerance of the cesium carbonate method for substituents attached to the 6-position of the pyrazinone, we first attempted the reaction with the 3-methyl-substituted pyrazinone **15** (Scheme 3). This was prepared by treatment of 2-[(4-methoxybenzyl)amino]propanenitrile **12** with oxalyl chloride to form **13**, followed by Stille coupling with tetramethyltin (**14**) and trifluoroacetic acid catalyzed removal of the *N*-(*p*-methoxybenzyl) protecting group (Scheme 3). It is noteworthy that the signals of the two methyl groups of **14** appear in the NMR spectrum as quadruplets with a rare ^7J value of ca. 1 Hz when the

Gaussian−Lorentz enhance function (lb: −2.0 Hz; gb: 0.5 Hz) is applied prior to the FID processing. Unfortunately, the undesired *O*-alkenylated compound **16** was isolated almost exclusively when **15** was heated with 5-bromo-1-pentene and Cs_2CO_3 in dioxane, demonstrating that selective *N*-alkenylation of 6-substituted pyrazinones is not feasible.

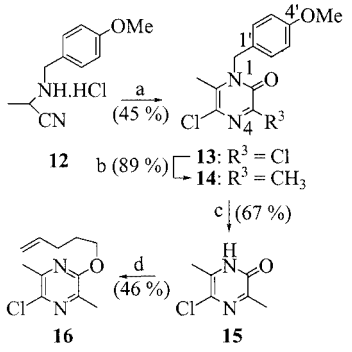

Scheme 3. a) $(COCl)_2$, $Et_3N{\cdot}HCl$, PhCl, room temp., 2 d; b) $Sn(CH_3)_4$, $[Pd(PPh_3)_4]$, toluene, 120 °C, 1 d; c) CF_3CO_2H, reflux, 10 h; d) $Br(CH_2)_3CH{=}CH_2$, Cs_2CO_3, dioxane, 50 °C, 5 d

To solve this *N*-alkenylation problem, we envisaged a different strategy based on the use of 5-(phenylselenyl)pentan-1-amine (**17**) as a substitute for direct incorporation of the acid-sensitive pent-4-en-1-amine into the pyrazinone ring system (Scheme 4). Amine **17** was converted into the corresponding aminonitrile **18** through a Strecker reaction with acetaldehyde, and the hydrochloride salt of crude **18** was treated with oxalyl chloride to provide the 3,5-dichloropyrazinone **19**. Subsequent Stille coupling with tetraphenyltin and $[Pd(PPh_3)_4]$ as a catalyst afforded the corresponding 3-phenyl derivative **20**, which was converted into **21** in high yield by application of a one-pot oxidation/elimination procedure with *m*CPBA. Intramolecular cycloaddition of **21** to form **22** proceeded more slowly than the analogous conversion of **7** (typically 7 d in refluxing PhBr) but with the same regioselectivity to provide bis(lactam) **23** upon hydrolysis of the intermediate imidoyl chloride adduct. As observed for bis(lactam) **9**, ^{13}C NMR analysis of **23** revealed the existence of a distorted nonplanar tertiary amide group (δ_{C2} = 179.0 ppm versus δ_{C10} = 171.2 ppm for the secondary amide) implying a ketone-like character for the carbonyl moiety and an increased basicity for N-3. Accordingly, selective acid-catalyzed solvolysis of the tertiary amide could again be effected by heating of **23** with 2.5 equiv. of methanesulfonic acid in methanol to furnish *cis*-1,7-naphthyridine **24** in almost quantitative yield (99%). The final conversion of amino ester **24** into the diamide **25** was carried out under the conditions described above for the preparation of the 8a-H analogue **11**.

Even though the synthesis of **25** is entirely diastereoselective, it still delivers two enantiomers. Both are potential β-turn mimics: the (4a*R*,6*S*,8a*R*) isomer, which mimics two L-amino acids upon deletion of the bridging elements, and the (4a*S*,6*R*,8a*S*) isomer, which mimics two conformationally constrained D-residues. While we were unable to separate

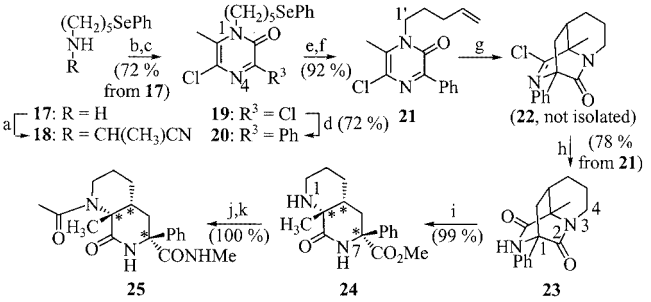

Scheme 4 . a) CH_3CHO, KCN, $NaHSO_3$, $MeOH/H_2O$, 60 °C, overnight; b) HCl bubbling, 0 °C, 15 min; c) $(COCl)_2$, $Et_3N{\cdot}HCl$, PhCl, room temp., 2 d; d) $SnPh_4$, $[Pd(PPh_3)_4]$, toluene, 120 °C, 7 d; e) *m*CPBA, CH_2Cl_2, −15 °C to room temp., 30 min; f) reflux, overnight; g) PhBr, reflux, 7 d; h) EtOAc satd. with H_2O, room temp., overnight; i) MeOH, 2.5 equiv. CH_3SO_3H, reflux, overnight; j) Ac_2O, 40 °C, 2 h; k) 33 wt% CH_3NH_2/EtOH, room temp., overnight

the enantiomers of amine precursor **24** by HPLC on a chiral stationary phase, we did succeed in analytical-scale separation of the bis(lactam) enantiomers **23** (see Exp. Sect.).

Conformational Analysis of Amines 10 and 24

Amino esters **10** and **24** predominantly exist as two opposite *cis*-fused conformers **10A** and **24B** as shown by the ^3J coupling values in the ^1H NMR spectra observed between the angular proton 4a-H and its vicinal protons 4-H and 5-H (Figure 2). The structure of **10A** was apparent from a large ^3J-*trans* value with 5-H_{ax} and a small ^3J-*gauche* value with both 4-H protons, while that of **24B** was characterized by a small ^3J-*gauche* value of about 5 Hz with both 5-H protons and a large ^3J-*trans* value with 4-H_{ax}. These conformational preferences were confirmed by modeling calculations by MM3* optimization in the gas phase and in $CHCl_3$ (Macromodel 5.0). Interestingly, opposite conformational preferences were demonstrated for the diamide

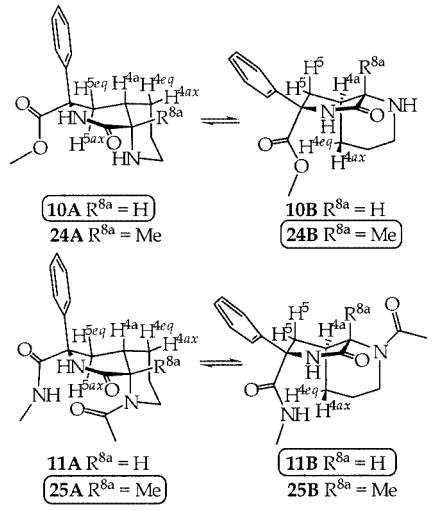

Figure 2. Conformational equilibria of *cis*-fused 1,7-naphthyridines favoring the opposite conformers **10A** and **24B** for the free amines or **11B** and **25A** for the diamides, according to ^1H NMR characterization and molecular modeling; the conformations detected by NMR are boxed

compounds **11** and **25** by the molecular modeling and the ^{1}H NMR spectroscopic data given below. Apparently, conformer **10B** is disfavored relative to **10A** by 1,3-diaxial repulsion between the ester group and C4, whereas in the favored conformer **24B** this effect is counterbalanced by the equatorial position of the 8a-Me group with respect to the piperidine chair moiety (conformer **24A** exhibits 1,3-diaxial repulsions between 8a-Me and 2-H_{ax} and 4-H_{ax}). In the analogous diamide conformer **25B**, such an equatorial 8a-Me group in turn meets a strong repulsion with the coplanar *N*-acetyl substituent, thus favoring the desired "closed" form **25A**. This repulsive effect is largely removed in the favored 8a-H diamide conformer **11B**, so that a similar but less severe repulsion (in relation to that in 8a-Me conformer **25B**) between the N−Ac amide bond and the coplanar equatorial 8−8a linkage in disfavored form **11A** comes into play.

Molecular Modeling of Diamides 11 and 25

To find the most relevant minimum-energy conformations of **11**, a random conformer search[11] and energy minimization were carried out with the Macromodel 5.0 AMBER* or MM3* force field in combination with the GB/SA solvation model (water). Ruling out improbable twist conformations, we identified three major structures **11A**−**C** in this way (Table 1). According to MM3* the lowest-energy conformer has the piperidinone ring in a half-chair conformation (**11B**), while AMBER* finds the (slightly deformed) piperidinone boat conformation **11C** to be lowest in energy. Conformer **11A**, with the desired β-turn structure, was found to be much higher in energy relative to the global minimum by MM3*, but only slightly higher according to AMBER*. To obtain improved energy data for the representative conformers **11A**−**C**, they were sub-

Table 1. Conformers of **11** in water and corresponding energies found by random conformer search by AMBER* and MM3*; these energies are compared to energies obtained by ab initio DFT calculations

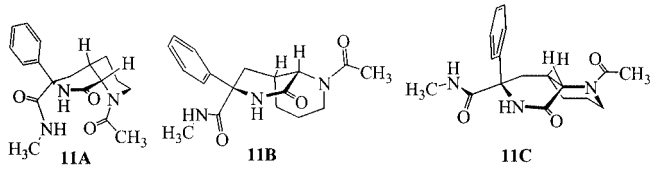

Conformer	Geometry optimization and hydration model [kJ/mol][a] AMBER*, GB/SA	MM3*, GB/SA	DFT[b][c]	DFT,[c] CPCM	DFT,[c] PCM
11A	1.05	17.06	18.70	20.12	22.59
11B	12.83	0.00	11.84	0.00	0.00
11C	0.00	1.66	0.00	11.93	17.74

[a] The global minimum energy is set to zero. [b] Gas phase. [c] B3LYP/6-31G**.

Table 2. Conformers of **25** in water and corresponding energies found by random conformer search by the AMBER* and MM3* methods; these energies are compared to energies obtained by ab initio DFT calculations

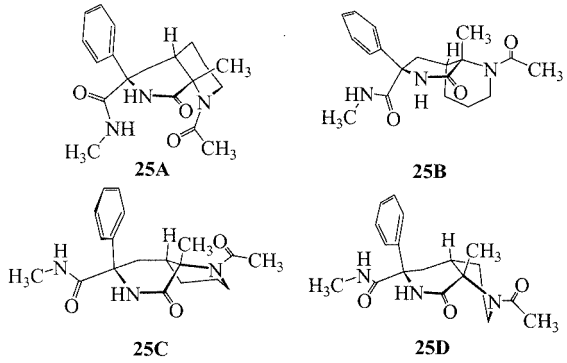

Conformer	Geometry optimization and hydration model [kJ/mol][a] AMBER*, GB/SA	MM3*, GB/SA	DFT[b][c]	DFT,[c] CPCM	DFT,[c] PCM
25A	0.00	0.00	0.00	0.00	0.00
25B	−[d]	2.49	22.54	13.25	11.45
25C[e]	45.53	31.90	25.11[e]	12.14	7.03
25D	31.77	1.32	24.18	14.73	7.49

[a] The global minimum energy is set to zero. [b] Gas phase. [c] B3LYP/6-31G**. [d] Not found by the conformer search. [e] Gas-phase DFT geometry optimization of **25C** gave a local minimum of conformer **25B** which was used in the CPCM and PCM hydration models.

mitted to DFT geometry optimization with the B3LYP functional in conjunction with the 6-31G** basis set. The results, summarized in Table 1, indicate that the lowest-energy conformer in the gas phase is **11C**. When the CPCM or PCM hydration models are used, however, the lowest-energy conformer is **11B**, in accordance with NMR analysis (see below).

The data described above indicate that the hydrogen-bonded conformer **11A** is sterically disfavored relative to the "open" forms **11B** and **11C**. However, the introduction of groups at the 8a-position could counterbalance steric effects in favor of the **A**-type conformation, due to the repulsion of the 8a-substituent with the co-planar *N*-acetyl group in the "open" forms of type **B** and **C**. This supposition was supported by an analogous computational analysis for 8a-methyl-1,7-naphthyridine **25** (Table 2). Random conformer searches by both the AMBER* and the MM3* force-field approaches yielded conformation **25A** as the global minimum, displaying properties conforming to the desired β-turn induction, including the generation of a hydrogen bond. The next two significantly different conformers identified by use of both force fields were **25D** and **25C**: the former is characterized by a twist-boat form of the piperidine moiety, while **25C** exhibits a piperidinone boat structure. Interestingly, conformer **25B** was not found by AMBER* but only when MM3* was used; however, a structure representing a local minimum of **25B** was generated by DFT geometry optimization of **25C** in the gas phase. After similar geometry optimization of **25A**, **B**, and **D**, the four optimized structures were subjected to further hydration energy calculations, which revealed **25A** as the most stable conformer by 7−12 kJ/mol depending on the hydration model used.

NMR Analysis of Diamides 11 and 25

^{1}H NMR spectra of **11** were run in $CDCl_3$, [D_6]DMSO and D_2O; the last spectrum gave the least overlap but no NH signal. In each case a series of separate signals revealed the existence of two slowly interconverting (*cis*,*trans*) rotamers about the N^1-Ac amide linkage. From the NOE enhancement observed for 2-H_{eq} upon presaturation of the *N*-Ac protons in the NOE difference spectra, the *trans* rotamer [(*Z*) form] was shown to be the main form in D_2O but not in [D_6]DMSO, in which strong dipolar interactions with the solvent may be involved. In all three solvents the *cis*-fused naphthyridine moiety apparently adopts a similar conformation corresponding to that of **11B**, as demonstrated by the relevant coupling constants for the angular proton 4a-H. The latter showed a small ^3J-*gauche* value of ca. 5 Hz with both 5-H protons and a large ^3J-*trans* value of ca. 14 Hz with 4-H_{ax}, in accordance with the coupling values calculated for **11B**.[12] The 2D NOESY spectrum in $CDCl_3$ or D_2O also displayed a weak correlation between the phenyl *ortho*-protons and proton 8a-H (Figure 3), indicating a partial orthogonal orientation of the phenyl ring relative to the piperidinone ring in **11B**.

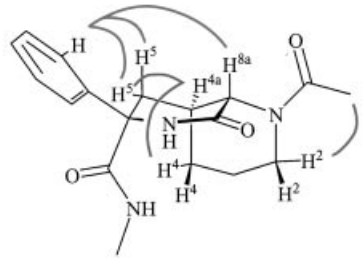

Figure 3. Solution conformation and relevant NOESY correlations (gray) of **11**

While conformer **11B** is not desired for β-turn induction, it seemed worthwhile to verify the criteria usually cited for intramolecular hydrogen-bonding analysis by NMR: (1) the temperature shift of the hydrogen-bonded proton is ≤ −3 ppb/°C, and (2) if the solvent is changed, a large shift is seen for free N*H* proton(s) and a small one for the hydrogen-bonded proton. By increasing the temperature from 298 to 343 K in steps of 5 K ([D_6]DMSO) an N*H*CH_3 temperature dependence of −2.9 and −3.8 ppb/K was determined for the two *N*-Ac rotamers (Figure 4). The fact that one of the N*H* proton signals seems to fulfil the criterion is deceptive, since the two signals coalesce at 333 K, giving rise to second-order effects and a deviation from linearity. The N^7H proton signals show a greater temperature dependence of −5.3 and −5.4 ppb/K. When [D_6]DMSO was exchanged for $CDCl_3$, large shifts were observed for all N*H* protons.

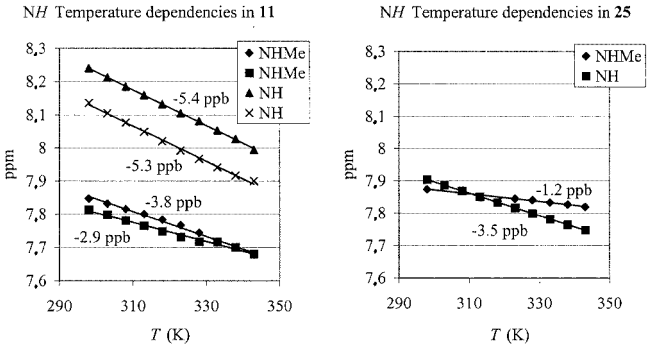

Figure 4. N*H* temperature dependence observed for **11** and **25**

In [D_6]DMSO, the appearance of the spectrum of **25** was totally unlike that of **11**. Only one *N*-acetyl rotamer was observed, and the spectrum also displayed a different multiplet structure for coupling of the angular proton 4a-H with the vicinal protons 5-H and 4-H. For example, 5-H_{ax} was observed as a triplet at δ = 2.41 ppm, corresponding to geminal coupling with 5-H_{eq} and *trans*-diaxial coupling with 4a-H ($^2J \approx {}^3J \approx 14$ Hz). This indicates an *axial* position of the angular proton 4a-H with respect to the piperidinone ring. 5-H_{eq} was observed as a broadened doublet, due to a very small (unresolved) coupling with 4a-H, at δ = 1.98 ppm. A *gauche* coupling value of ca. 6 Hz was meas-

ured between 4a-H and 4-H_{ax}, which appeared as a triplet of triplets (4-H_{eq} signal hidden). These coupling values clearly support **25A** as the predominant conformation. Since an intramolecular hydrogen bond was indicated by the conformational calculations carried out for favored conformer **25A**, diamide **25** was submitted to the NMR criteria described above. When the solvent was changed from [D_6]DMSO to $CDCl_3$, the signal of the N*H* proton of the piperidinone ring was shifted from δ = 7.88 ppm to δ = 6.42 ppm, while the signal of the N*H*Me proton did not move significantly (from δ = 7.80 ppm to δ = 7.85 ppm). As expected for hydrogen bonding of the N*H*Me proton, the N*H* temperature dependence was only −1.2 ppb/K for N*H*Me, versus −3.5 ppb/K for the piperidinone amide proton.

Additional support for conformation **25A** was obtained from the NOESY spectrum ([D_6]DMSO). As illustrated in Figure 5, strong NOEs were found between (amongst others): (1) the *ortho*-protons of the phenyl group and 4a-H/5-H_{eq}, (2) N*H*Me and 5-H_{ax}, (3) 2-H_{ax} and 8a-CH_3, and (4) *N*$COCH_3$ and 2-H_{eq}. These correlations confirm the existence of conformer **25A**.

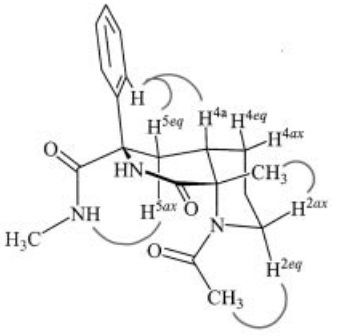

Figure 5. Solution conformation ([D_6]DMSO) and relevant NOESY correlations (gray) of **25**

Evaluation of β-Turn-Inducing Potential

Relevant structural features of mimics **1** and **2** may be compared to those of rigidified *cis*-amide mimics constrained in a six-membered lactam ring, such as the monocyclic lactam **26**,[7a] and the 5(1*H*)-indolizinone mimic **27** (Figure 6).[7b] A good overlay was observed for the backbones of **1** and **2** and the mono- and bicyclic lactam structures **26** and **27** (Macromodel 5.0, MM3*-optimized structures), suggesting that these compounds may have similar β-turn-inducing properties.[13] Like other turn mimics that conformationally constrain or isosterically replace the central dipeptide backbone, lactam compounds **1** and **2** can be defined as *external* β-turns.[14] These can be compared to *internal* β-turns, which try to mimic the whole β-turn tetrapeptide without explicitly considering the backbone geometry. Generally, external β-turn mimics are more rigid, but are often unable to mimic amino acid side chains.

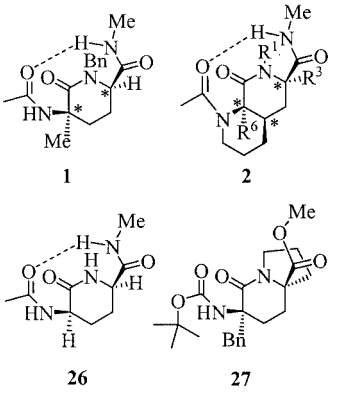

Figure 6. Compounds **1** and **2** in comparison with previously reported type VI β-turn mimics **26** and **27**

However, in comparison with the previously described external mimics (e.g., **26** and **27**), an asset of the naphthyridine-type mimic **2** is that it can be variably functionalized at the stereogenic Cα2 and Cα3 positions bearing the angular R^3 and R^6 substituents, thus allowing for modulation of receptor−ligand interactions. From a molecular recognition perspective, the classification of β-turns as types I−VII according to the dihedral angles of the central residues is not entirely satisfactory, since it does not adequately describe the disposition of the Cα2 and Cα3 substituents and the orientation of the *i* and *i*+3 residues representing the positions at which the peptide chain would enter and exit the β-turn, respectively. To solve this problem, the topographies of β-turns and their mimics can be described in terms of a single virtual torsion angle β, defined by C1, Cα2, Cα3, and N4 of the tetrapeptide model and the interatomic distance *d* between Cα1 and Cα4 (Ball et al.[15]). The collection of naturally occurring β-turns (type I, II, ...) examined by Ball has a broad distribution of β-values (roughly ±100° with a slight preference for small, positive β values). It therefore seems relevant to "match" the β value of the mimic with that of the target peptide. For type VI turns, however, a much narrower β value (−19° < β < 20°) was found. We can therefore use this interval as a boundary for the β value of a type VI turn mimic. Thus, the DFT geometry-optimized global minimum **25A** was evaluated as a tight reverse turn inducer based on three geometrical criteria (Figure 7): (1) the virtual torsion angle β should be within 0±20°, (2) the Cα1−C4 interatomic distance *d* should be less than or equal to 7 Å, and (3) the distance between the *N*-acetyl carbonyl oxygen atom and the methyl carboxamide proton should be smaller than 2.5 Å and the NH−O and H−OC angles greater than 120 and 90°, respectively (hydrogen bonding). All of these criteria are fulfilled by the tetrapeptide model: the |β| value measured for (4a*R*,6*S*,8a*R*)-**25A** was 16° [and concurrently, for (4a*S*,6*R*,8a*S*)-**25A**, −16°], the Cα1−Cα4 interatomic distance was 5.5 Å, and the

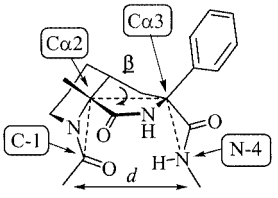

Figure 7. The virtual torsion angle β and the Cα1−Cα4 interatomic distance *d* measured for (4a*R*,6*S*,8a*R*)-**25A**

NH−O=C distance was 2.0 Å. The NH−O and H−OC angles measured were 155 and 143°, respectively. Hence, these data clearly support the β-turn-inducing properties of **25A**.

The picture described above is somewhat idealized, since several low-energy conformations equilibrate with **25A** at room temperature. To assess the contributions of all conformations that fulfil the conditions for reverse-turn induction, a molecular dynamics simulation of 1600 ps at 300 K in water was carried out for **25** by use of AMBER 6.0 and the TIP3P water model. In this way, 8000 snapshots were generated, from which the β values and Cα1−Cα4 distances *d* could be extracted. As can be seen from the results summarized in Table 3, 66% of the conformations have a β within ±20° and 87% have a *d* value below 7 Å. According to our proposed hydrogen-bond conditions, 25% of all conformations are hydrogen-bonded and 67% of the conformations have an NH−O=C distance of less than 4 Å (with the same angle conditions), the minimum distance usually cited for significant interaction. These results indicate that **25** largely preserves its β-turn-inducing properties at 300 K in water.

Table 3. Parameters extracted from a molecular dynamics simulation of **25**

Property	Compound **25**
β within ±20°	66%
Mean β (4a*R*,6*S*,8a*R*)-**25A**	(17 ± 8)°
Mean β (4a*S*,6*R*,8a*S*)-**25A**	(−17 ± 8)°
d within 7 Å	87%
Mean *d*	6.1 Å
H-bonded	25%
NH−O=C interaction	67%

In this context, it should be noted that in a conformational study using a molecular dynamics simulation in which several β-turn mimetics were built into cyclic Ala-hexapeptides,[16] the rigid *cis*-amide **27** was shown to be compatible with the opposing β-turn in the ring, which was not the case for a biphenyl-based mimic. Also, in a Monte Carlo simulation, **27** displayed the best β-turn-inducing potential, including the generation of a H-bridge between the *i* and *i*+3 residues. In this simulation, distribution profiles of the following properties were generated: (a) the donor−acceptor distance (HN_{i+3})−($C{=}O_i$) of the turn-stabilizing bond, b) the C*α*i−C*α*i+3 distance characteristic of β-turns (ideal value: 4.1−4.8 Å), according to Lewis et al.,[17] and c) the pseudodihedral angle encompassing four consecutive Cα atoms of the turn-forming amino acids or dipeptide analogues (ideal value: 50° > Θ > −50°). The ideal values were taken from the geometries of known β-turns. A narrow distribution was considered important for β-turn-inducing properties.

When an analogous molecular dynamics simulation was performed on a cyclic Ala-hexapeptide in which (4a*S*,6*R*,8a*S*)-**25** and (4a*R*,6*S*,8a*R*)-**25** were incorporated (Macromodel 8.0, GB/SA hydration model), these structures were also found to adopt stable conformations, each with two β-turns. A molecular dynamics simulation was also carried out on linear Ac−Ala−Ala−(4a*R*,6*S*,8a*R*)-**25**−Ala−Ala−NHMe and Ac−Ala−Ala−(4a*S*,6*R*,8a*S*)-**25**−Ala−Ala−NHMe. This resulted in narrow distribution profiles similar to those found for **27** by use of the parameters described above (Figure 8). Moreover, 94% of the (4a*R*,6*S*,8a*R*)-**25**-hexapeptide and 81% of the (4a*S*,6*R*,8a*S*)-**25**-hexapeptide was found to be intramolecularly hydrogen-bonded (NH−O=C distance < 2.5 Å; NH−O angle > 120°; H−OC angle > 90°).

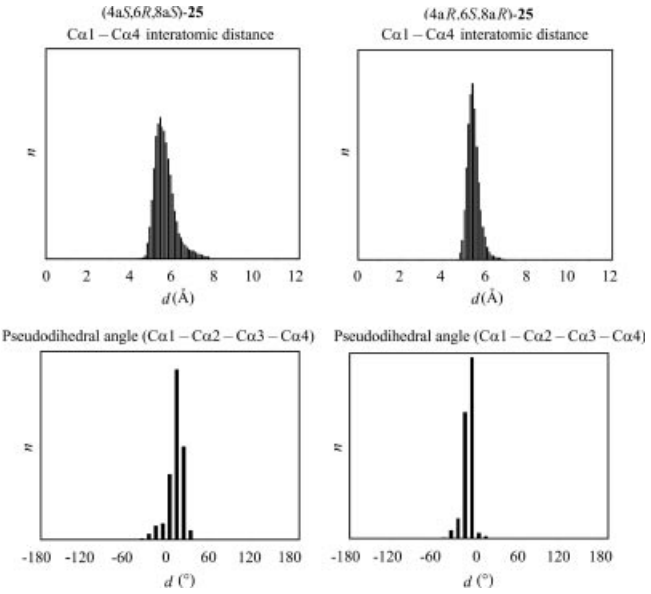

Figure 8. Interatomic distances C*α*i−C*α*i+3 and pseudodihedral angles C*α*i−C*α*i+1−C*α*i+2−C*α*i+3 for both enantiomers of the β-turn-induced by **25** in an Ala-hexapeptide; values determined by an MD simulation (force field AMBER*, solvent H_2O)

Conclusion

The intramolecular Diels−Alder reaction of *N*-alkenyl-2(1*H*)-pyrazinones, followed by cleavage of the strained tricyclic adducts to form *cis*-fused 1,7-naphthyridines, can be used to construct a novel type of rigid β-turn. Substitution at the 8a-position of the *cis*-fused naphthyridine scaffold proved to be of crucial importance for attaining the desired conformation, as indicated by random conformer searches, ab initio geometry optimizations, and molecular dynamics conformational space probing around the global minimum. The presumed existence of **25A** as the predominant conformer required for induction of β-turns and internal hydrogen bonding was confirmed by extensive NMR analysis. In comparison with the previously described *cis*-amide mimics **26** and **27**, an additional asset of type **2** mimics is that they can be variably functionalized at the stereogenic Cα2 and Cα3 positions, which should allow for further modulation of the receptor−ligand interaction.

Experimental Section

General Remarks: All compounds were analyzed with the analytical instruments described previously.[18] NMR spectra were calibrated

with TMS, except for **11** in D_2O (HOD) and **25** in [D_6]DMSO (CHD_2SOCD_3). For **11**, only the ^{1}H NMR spectroscopic data of major isomers are given.

Random Conformer Searches: The calculations were carried out with Macromodel 5.0.[19] The Macromodel implementation of the AMBER force field (denoted AMBER*)[20] was used with the water GB/SA solvation model of Still et al.[21] The conformational space was sampled by use of Goodman and Still's internal coordinate Monte Carlo search.[22] For both molecules (**11** and **25**), 5000 structures were generated and minimized to an energy convergence of 0.05 kJ/mol Å by use of the Polak−Ribiere conjugate gradient method implemented in Macromodel. Duplicate structures and those greater than 50 kJ/mol above the global minimum were discarded.

Ab Initio Geometry Optimization: Gas-phase geometry optimizations were performed at the Density Functional Theory level in combination with the B3LYP functional level in conjunction with the d,p polarized basis sets 6-31G**. Hydration energies were calculated by use of the polarizable continuum model (PCM) developed by Tomasi and co-workers.[23] A second solvation model used is CPCM,[24] which is actually an implementation of the Conductor-like Screening Model (COSMO).[25] The hydration free energies were calculated at the HF/6-31G** level. The United Atom Model for Hartree Fock (UAHF) definition[26] was used for the construction of the solute cavity. No geometry optimizations in solvent were performed for the hydration free energies; the calculated gas-phase structures were used. All calculations were performed with the aid of the Gaussian 98 package.[27]

Molecular Dynamics of 25: The simulation was performed at constant temperature (300 K) and constant pressure (1 atm) by use of the SANDER classic module of AMBER 6.0 with the AMBER force-field of Cornell et al.[28] This was slightly modified to handle the unnatural residue, and Mulliken charges from the DFT calculations were used instead of the standard values. An initial solvent box of ca. 37 × ca. 34 × ca. 31 Å, containing 866 TIP3P water molecules,[29] was constructed around the residue. The system was minimized until the rms energy gradient dropped below 0.1 kcal/mol·Å. After a relaxation period, the simulation was subsequently run for 1600 ps with SHAKE on all bond lengths and with a time step of 0.002 ps. Periodic boundary conditions were used to treat the nonbonded interactions with a cut-off distance equal to 9 Å. Snapshots were taken every 0.2 ps, yielding 8000 conformations for analysis.

Molecular Dynamics of Ala-Hexapeptides with 25: Molecular dynamics simulations on cyclo(Ala−Ala-**25**−Ala−Ala) and the linear peptide Ac−Ala−Ala-**25**-Ala−Ala−NHMe (all non-β-turn mimic peptide bonds in the *trans* conformation) were performed with the Macromodel 8.0 package with use of the AMBER* force field. The run was set up with all standard parameters and the GB/SA solvation model (water).[21] The system was minimized and after an equilibration run of 200 ps, a 1000 ps dynamics run was performed (timestep 1 fs). The criteria described above were monitored. For the linear peptide, an extended and a near-ideal β-turn structure were chosen as a starting conformation. The reported data are from the near-ideal starting conformation. In the case of the extended starting conformation, results were considerably poorer for a 1000 ps run with 200 ns equilibration. When a longer equilibration time (1000 ps) was used, however, the results became similar to the reported data, 91% of Ac−Ala−Ala−(4a*R*,6*S*,8a*R*)-**25**-Ala−Ala−NHMe and 87% of Ac−Ala−Ala-(4a*S*,6*R*,8a*S*)-**25**-Ala−Ala−NHMe being hydrogen-bonded.

3,5-Dichloro-1-(4-methoxybenzyl)-2(1*H*)-pyrazinone (4): The product was prepared as described in ref.[9], starting from 4-methoxybenzylamine (26.1 mL, 0.2 mol). Yield: 29.0 g (51%), yellow crystals; m.p. 96−100 °C (EtOH). IR (KBr, cm^{-1}): $\tilde{\nu}$ = 1662.8 (C=O), 1588.7 (C=N). ^{1}H NMR (400 MHz, $CDCl_3$): δ = 7.28 (m, 2 H, 3′-H, 5′-H), 7.15 (s, 1 H, 6-H), 6.92 (m, 2 H, 2′-H, 6′-H), 5.03 (s, 2 H, CH_2), 3.82 (s, 3 H, CH_3) ppm. ^{13}C NMR (100 MHz, $CDCl_3$): δ = 159.9 (C-4′), 151.5 (C-2), 147.0 (C-3), 130.3 (C-2′, C-6′), 125.6, 125.1 (C-6, C-5), 123.8 (C-1′), 114.6 (C-3′, C-5′), 55.2 (CH_3), 52.3 (CH_2) ppm. MS EI: *m*/*z* (%) = 284 (5) [M^+], 121 (100) [$CH_3OC_6H_4CH_2^+$]; exact mass calculated for $C_{12}H_{10}Cl_2N_2O_2$ 284.0119; found 284.0138.

5-Chloro-1-(4-methoxybenzyl)-3-phenyl-2(1*H*)-pyrazinone (5): The product was prepared as described in ref.[10], starting from **4** (10.0 g). Yield: 9.0 g (78%); yellow crystals; m.p. 84 °C (Et_2O). IR (KBr, cm^{-})^1: $\tilde{\nu}$ = 1640.4 (CO), 1585.4 (C=N). ^{1}H NMR (300 MHz, $CDCl_3$): δ = 8.36 (m, 2 H, *ortho*-H), 7.43 (m, 3 H, *meta*-H, *para*-H), 7.29 (d, *J* = 8 Hz, 2 H, 3′-H, 5′-H), 7.15 (s, 1 H, 6-H), 6.88 (d, *J* = 8 Hz, 2 H, 2′-H, 6′-H), 5.02 (s, 2 H, CH_2), 3.78 (s, 3 H, CH_3) ppm. ^{13}C NMR (75 MHz, $CDCl_3$): δ = 159.9 (C-4′), 154.3 (C-2), 152.0 (C-3), 134.8 [C-*ipso* (Ph)], 130.5, 129.2, 128.0 [C-*ortho*, C-*meta*, C-*para* (Ph)], 130.3 (C-2′, C-6′), 126.3, 126.2 (C-1′, C-5), 125.1 [C-6 (determined by DEPT)], 114.5 (C-3′, C-5′), 55.2 (CH_3), 52.3 (CH_2) ppm. MS EI: *m*/*z* (%) = 326 (9) [M^+], 121 (100) [$CH_3OC_6H_4CH_2^+$]; exact mass calculated for $C_{18}H_{15}ClN_2O_2$ 326.0822; found 326.0829.

5-Chloro-3-phenyl-2(1*H*)-pyrazinone (6): Compound **5** (9.0 g) was added to trifluoroacetic acid (30 mL). This solution was stirred at reflux for 5 h [TLC monitoring: R_f (CH_2Cl_2) = 0.31 (**5**), 0.10 (**6**)]. After evaporation of the solvent, crude **6** was purified by column chromatography (silica gel, CH_2Cl_2 to 15% EtOAc/CH_2Cl_2). Yield: 5.0 g (88%); yellow crystals; m.p. 175 °C (EtOAc/CH_2Cl_2). IR (KBr, cm^{-1}): $\tilde{\nu}$ = 2692 (broad, NH), 1648 (C=O), 1590.7 (C=N). ^{1}H NMR (400 MHz, [D_6]DMSO):[30] δ = 8.10 (m, 2 H, *ortho*-H), 7.67 (s, 1 H, 6-H), 7.40 (m, 3 H, *meta*-H, *para*-H) ppm. ^{13}C NMR (100 MHz, [D_6]DMSO): δ = 155.4 (C-2), 148.5 (C-3), 135.1 (C-*ipso*), 130.6 (C-*para*), 129.3 (C-6), 128.9, 128.6 (C-*ortho*, C-*meta*) ppm; C-5 signal not resolved. MS EI: *m*/*z* (%) = 206 (100) [$M^{+\cdot}$], 178 (74) [$M^{+\cdot}$ − CO], 143 (33) [$M^{+\cdot}$ − CO − Cl], 116 (33) [$M^{+\cdot}$ − CO − Cl − HCN]; exact mass calculated for $C_{18}H_{15}ClN_2O_2$ 206.0247; found 206.0254.

5-Chloro-1-(4-pentenyl)-3-phenyl-2(1*H*)-pyrazinone (7): Cs_2CO_3 (1.9 g, 1.2 equiv.) was added to a solution of **6** (4.0 g) in dioxane (150 mL). This mixture was stirred at 50 °C for 30 min, followed by addition of 5-bromo-1-pentene (0.9 mL, 1.5 equiv.). After having been stirred for one week, the mixture was filtered to remove CsBr and unchanged Cs_2CO_3. After evaporation of the solvent, crude **7** was purified by column chromatography (silica gel, CH_2Cl_2). Yield: 3.8 g (72%); yellow oil. IR (NaCl, cm^{-1}): $\tilde{\nu}$ = 1650.1 (C=O), 1583.5 (C=N). ^{1}H NMR (400 MHz, $CDCl_3$): δ = 8.35 (m, 2 H, *ortho*-H), 7.43 (m, 3 H, *meta*-H, *para*-H), 7.18 (s, 1 H, 6-H), 5.80 (ddt, *J* = 18, 10, 7 Hz, 1 H, 4′-H), 5.06 (m, 2 H, 5′-H), 3.93 (t, *J* = 7 Hz, 2 H, 1′-H), 2.15 (q, *J* = 7 Hz, 2 H, 3′-H), 1.90 (quint, *J* = 7 Hz, 2 H, 2′-H) ppm. ^{13}C NMR (100 MHz, $CDCl_3$): δ = 154.3 (C-2), 152.0 (C-3), 136.5 (C-4′), 134.8 (C-*ipso*), 130.6, 129.2, 128.1 (C-*ortho*, C-*meta*, C-*para*), 126.2 (C-5), 125.9 (C-6), 116.2 (C-5′), 50.1 (C-1′), 30.5, 27.5 (C-2′, C-3′) ppm. MS EI: *m*/*z* (%) = 274 (100) [$M^{+\cdot}$], 220 (92) [$M^{+\cdot}$ − C_4H_6], 191 (50) [$M^{+\cdot}$ − C_4H_6 − CHO); exact mass calculated for $C_{15}H_{15}ClN_2O$ 274.0873; found 274.0873.

1-Phenyl-3,10-diazatricyclo[5.3.1.0^{3,8}]undecane-2,9-dione (9): A solution of **7** (1.0 g) in bromobenzene (20 mL) was stirred at reflux

overnight. The solvent was then evaporated, and the residue was redissolved in water-saturated ethyl acetate. The mixture was stirred overnight and pure **9** was collected by filtration. Yield: 0.80 g (86%). For spectroscopic data see ref.[8]

Methyl 8-Oxo-6-phenyldecahydro[1,7]naphthyridine-6-carboxylate (10): Methanesulfonic acid (95 μL, 2.5 equiv.) was added to a solution of **9** (150 mg, 0.52 mmol) in MeOH. This solution was stirred at reflux overnight. After evaporation of the solvent, 10% K_2CO_3 in water and CH_2Cl_2 were added to the residue. The organic phase was separated and the aqueous phase was extracted three times with CH_2Cl_2. The combined organic layers were dried with anhydrous K_2CO_3. Pure **10** was obtained after filtration and removal of the solvent. Yield: 164 mg (97%). For spectroscopic data see ref.[8]

1-Acetyl-*N*-methyl-8-oxo-6-phenyldecahydro[1,7]naphthyridine-6-carboxamide (11): Compound **10** (110 mg, 0.38 mmol) was dissolved in acetic anhydride (20 mL). After having been stirred at 40 °C for 2 h, the solution was concentrated to dryness and the residue was redissolved in a solution of CH_3NH_2 in ethanol (20 mL, 33wt%). This solution was stirred at room temp. overnight and concentrated, and the residue was purified by chromatography on preparative plates (5% MeOH/CH_2Cl_2) to yield **11** (118 mg, 0.36 mmol). Yield: 94%; white crystals, m.p. 115−120 °C (Et_2O). IR (KBr, cm^{-1}): $\tilde{\nu}$ = 1666.2 (C=O), 1546.4 (C=O). **(*Z*) Isomer (74%):** ^{1}H NMR (400 MHz, $CDCl_3$): δ = 8.18 (s, 1 H, 7-H), 7.49−7.26 (m, 5 H, arom. H), 6.81 [m (q), 1 H, N*H*CH_3], 5.30 (d, *J* = 5 Hz, 1 H, 8a-H), 3.58 (br. d, *J* = 14 Hz, 1 H, 2-H_{eq}), 3.06 (dd, *J* = 14, 3 Hz, 1 H, 5-H_{eq}), 2.83 (td, *J* = 13, 2.5 Hz, 1 H, 2-H_{ax}), 2.79 (d, *J* = 5 Hz, 3 H, NHC*H*$_3$), 2.22 (dd, *J* = 14, 5 Hz, 1 H, 5-H_{ax}), 2.08 (m, 1 H, 4a-H), 2.05 (s, 3 H, $COCH_3$), 1.88 (m, 1 H, 4-H_{eq}), 1.69 (m, 1 H, 3-H_{eq}), 1.39 (qt, *J* = 13, 3.5 Hz, 1 H, 3-H_{ax}), 1.23 (m, 1 H, 4-H_{ax}) ppm. **(*E*) Isomer (58%):** ^{1}H NMR ([D_6]DMSO): δ = 8.23 (s, 1 H, 7-H), 7.84 [q (broad), *J* = 4 Hz, 1 H, N*H*CH_3], 7.44−7.27 (m, 5 H, arom. H), 4.56 (d, *J* = 5 Hz, 1 H, 8a-H), 4.25 (br. d, *J* = 14 Hz, 1 H, 2-H_{eq}), 3.01 (br. d, *J* = 13 Hz, 1 H, 5-H_{eq}), 2.64 (d, *J* = 5 Hz, 3 H, NHC*H*$_3$), 2.13 (m, 3 H, 2-H_{ax}, 4a-H, 5-H_{ax}), 1.94 (s, 3 H, $COCH_3$), 1.70−1.10 (m, 4 H, 3-H, 4-H) ppm. **(*Z*) Isomer (68%):** ^{1}H NMR (400 MHz, D_2O): δ = 7.61−7.49 (m, 5 H, arom. H), 5.29 (d, *J* = 6 Hz, 1 H, 8a-H), 3.95 (br. d, *J* = 14 Hz, 1 H, 2-H_{eq}), 2.97 (td, *J* = 13, 2 Hz, 1 H, 2-H_{ax}), 2.87 (s, 3 H, $NDCH_3$), 2.80 (dd, *J* = 15, 6 Hz, 1 H, 5-H_{eq}), 2.72 (dd, *J* = 15, 5 Hz, 1 H, 5-H_{ax}), 2.35 (m, 1 H, 4a-H), 2.27 (s, 3 H, $COCH_3$), 1.93 (m, 1 H, 4-H_{eq}), 1.83 (m, 1 H, 3-H_{eq}), 1.57 (qt, *J* = 13, 3.5 Hz, 1 H, 3-H_{ax}), 1.35 (qd, *J* = 13, 3 Hz, 1 H, 4-H_{ax}) ppm. **(*Z*) Isomer:** ^{13}C NMR (100 MHz, $CDCl_3$): δ = 171.9, 170.7, 170.5 (C=O), 142.4 (C-*ipso*), 129.0, 128.1, 124.8 (C-*ortho*, C-*meta*, C-*para*), 65.1 (C-6), 52.7 (C-8a), 43.6 (C-2), 38.1 (C-5), 33.0 (C-4a), 27.2 ($NHCH_3$), 27.1, 25.4 (C-3, C-4), 21.4 (CO*C*H$_3$) ppm. **(*E*) Isomer:** most signals not resolved. MS EI: *m*/*z* (%) = 329 (6) [$M^{\cdot+}$], 286 (18) [$M^{\cdot+}$ − Ac], 271 (100) [$M^{\cdot+}$ − $CONHCH_3$], 229 (26) [$M^{\cdot+}$ − CH_2O − $CONHCH_3$], 152 (62) [**8** − $H_{10}NO_2^+$], 96 (18) [$C_6H_{10}N^+$], 83 (16) [$C_5H_9N^+$]; exact mass calculated for $C_{18}H_{23}N_3O_3$ 329.1739; found 329.1735.

3,5-Dichloro-1-(4-methoxybenzyl)-6-methyl-2(1*H*)-pyrazinone (13): The product was prepared as described in ref.[9], starting from 4-methoxybenzylamine (26.1 mL, 0.2 mol). Yield: 26.8 g (45%); white crystals, m.p. 112 °C (EtOH). IR (KBr, cm^{-1}): $\tilde{\nu}$ = 1667.2 (C=O), 1567.6 (C=N). ^{1}H NMR (300 MHz, $CDCl_3$): δ = 7.16 (d, *J* = 9 Hz, 2 H, 3′-H, 5′-H), 6.87 (d, *J* = 9 Hz, 2 H, 2′-H, 6′-H), 5.30 (s, 2 H, CH_2), 3.79 (s, 3 H, OCH_3), 2.45 (s, 3 H, 6-CH_3) ppm. ^{13}C NMR (75 MHz, $CDCl_3$): δ = 159.6 (C-4′), 153.1 (C-2), 143.7 (C-3), 136.0 (C-1′), 128.6 (C-3′, C-5′), 125.9, 123.8 (C-5, C-6), 114.5 (C-2′, C-6′), 55.3 (OCH_3), 49.7 (CH_2), 16.8 (6-*C*H$_3$) ppm. MS EI: *m*/*z* (%) = 298 (4) [$M^{\cdot+}$], 121 (100) [$CH_3OC_6H_4CH_2^+$]; exact mass calculated for $C_{13}H_{12}Cl_2N_2O_2$ 298.0276; found 298.0280.

5-Chloro-1-(4-methoxybenzyl)-3,6-dimethyl-2(1*H*)-pyrazinone (14): The product was prepared as described in ref.[10], starting from **13** (10.0 g). Yield: 8.3 g (89%), brown crystals (CH_2Cl_2), m.p. 113−114 °C (CH_2Cl_2). IR (KBr, cm^{-1}): $\tilde{\nu}$ = 1647.5 (C=O), 1572.3 (C=N). ^{1}H NMR (300 MHz, $CDCl_3$): δ = 7.13 (d, *J* = 9 Hz, 2 H, 3′-H, 5′-H), 6.85 (d, *J* = 9 Hz, 2 H, 2′-H, 6′-H), 5.25 (s, 2 H, CH_2), 3.78 (s, 3 H, OCH_3), 2.48 (q, *J* = 1 Hz, 3 H, 3-CH_3)[31], 2.40 (q, *J* = 1 Hz, 3 H, 6-CH_3)[31] ppm. ^{13}C NMR (75 MHz, $CDCl_3$): δ = 159.3 (C-4′), 156.2 (C-2), 154.2 (C-3), 133.2 (C-1′), 128.3 (C-3′, C-5′), 126.7, 125.5 (C-5, C-6), 114.3 (C-2′, C-6′), 55.2 (OCH_3), 48.1 (CH_2), 20.7 (3-CH_3), 16.6 (6-CH_3) ppm. MS EI: *m*/*z* (%) = 278 (11) [$M^{\cdot+}$], 121 (100) [$CH_3OC_6H_4CH_2^+$]; exact mass calculated for $C_{14}H_{15}ClN_2O_2$ 278.0822; found 278.0826.

5-Chloro-3,6-dimethyl-2(1*H*)-pyrazinone (15): The same procedure as employed for compound **6** was used, starting from **14** (5.0 g). Yield: 1.9 g (67%); white crystals, decompose upon heating. IR (KBR, cm^{-1}): $\tilde{\nu}$ = 1651.5 (C=O), 1532.7 (C=N). ^{1}H NMR (300 MHz, $CDCl_3$): δ = 12.32 (br. s, 1 H, 1-H), 2.25 (s, 3 H, 3-CH_3 or 6-CH_3), 2.23 (s, 3 H, 6-CH_3 or 3-CH_3) ppm. ^{13}C NMR (75 MHz, [D_6]DMSO): δ = 157.4 (C-2); C-3, C-5, C-6 signals not resolved due to tautomerism, 20.1 (3-CH_3), 18.4 (6-CH_3) ppm. MS EI: *m*/*z* (%) = 158 (99) [$M^{\cdot+}$], 130 (59) [$M^{\cdot+}$ − CO], 129 (100) [$M^{\cdot+}$ − CO − H]; exact mass calculated for $C_6H_7ClN_2O$ 158.0247; found 158.0265.

2-Chloro-3,6-dimethyl-5-(4-pentenyloxy)-2(1*H*)-pyrazinone (16): The same procedure as employed for compound **7** was used, starting from **15** (1.0 g). Yield: 0.66 g (46%); colorless oil. IR (NaCl, cm^{-1}): $\tilde{\nu}$ = 1641.2 (C2=N1), 1543.2 (C3=N4) ppm. ^{1}H NMR (300 MHz, $CDCl_3$): δ = 5.84 (ddt, *J* = 18, 10, 7 Hz, 1 H, 4′-H), 5.04 (m, 2 H, 5′-H), 4.31 (t, *J* = 7 Hz, 2 H, 1′-H), 2.47 (s, 3 H, 3-CH_3), 2.40 (s, 3 H, 6-CH_3), 2.23 (q, *J* = 7 Hz, 2 H, 3′-H), 1.89 (quint, *J* = 7 Hz, 2 H, 2′-H) ppm. ^{13}C NMR (300 MHz, $CDCl_3$): δ = 156.6 (C-2), 145.2 (C-3), 140.9 (C-5), 137.6 (C-4′), 137.1 (C-6), 115.1 (C-5′), 65.9 (C-1′), 30.1 (C-3′), 27.9 (C-2′), 21.1 (3-CH_3), 18.2 (6-CH_3) ppm. MS EI: *m*/*z* (%) = 226 (16) [$M^{\cdot+}$], 158 (100) [$M^{\cdot+}$ − C_5H_8], 130 (18) [$M^{\cdot+}$ − C_5H_8 − CO], 68 (10) [$C_5H_8^+$]; exact mass calculated for $C_{11}H_{15}ClN_2O$ 226.0873; found 226.0874.

5-(Phenylselanyl)pentan-1-amine (17): This compound was prepared as described previously, starting from diphenyl diselenide (25 g).[32]

2-{[5-(Phenylselanyl)pentyl]amino}propanenitrile (18): The product was prepared by a previously described procedure,[33] starting from the amine (7.0 g, 28.9 mmol) at 60 °C and with a reaction time of 12 h. The compound was used for the preparation of **19** without purification.

3,5-Dichloro-6-methyl-1-[6-(phenylselanyl)pentyl]-2(1*H*)-pyrazinone (19): HCl was bubbled for 15 min through an ethereal solution of **18** (ca. 28.9 mmol). The mixture was then concentrated to dryness and the residue was suspended in dry CH_2Cl_2 (100 mL). Oxalyl chloride (6.0 mL, 69.1 mmol) in dry CH_2Cl_2 (100 mL) was added to this suspension with stirring. After 30 min, dry triethylammonium chloride (19.7 g, 144.0 mmol) was added, and the mixture was stirred at room temperature under N_2 for additional 2 d. After evaporation of the solvent and unchanged oxalyl chloride, the residue was purified by column chromatography (silica gel, CH_2Cl_2) to afford **19**. Yield: 8.4 g (72%) from **17**; yellow crystals, m.p. 68−71 °C (CH_2Cl_2). IR (KBr, cm^{-1}): $\tilde{\nu}$ = 1667.5 (C=O), 1567.8 (C=N). ^{1}H NMR (300 MHz, $CDCl_3$): δ = 7.48 (m, 2 H, *ortho*-H)

7.26−7.24 (m, 3 H, *meta*-H, *para*-H), 4.03 (m, 2 H, 1′-H), 2.91 (t, J = 7 Hz, 2 H, 5′-H), 2.46 (s, 3 H, CH_3), 1.78−1.66 (m, 4 H, 2′-H, 4′-H), 1.53 (quint, J = 7 Hz, 2 H, 3′-H) ppm. ^{13}C NMR (75 MHz, $CDCl_3$): δ = 152.5 (C-2), 143.4 (C-3), 135.2 (C-*ipso*), 132.5 (C-*ortho*), 130.0 (C-5), 129.0, 126.9 (C-*meta*, C-*para*), 123.7 (C-6), 47.2 (C-1′), 29.5 (C-2′), 27.2, 27.3, 26.7 (C-3′, C-4′, C-5′), 16.4 (CH_3) ppm. MS EI: *m*/*z* (%) = 404 (8) [$M^{\cdot+}$], 247 [$M^{\cdot+}$ − SePh], 192 (28) [$M^{\cdot+}$ − $C_{10}H_{12}Se$], 178 (81) [$M^{\cdot+}$ − $C_{11}H_{14}Se$], 156 (22) [$PhSe^+$], 77 (24) [Ph^+], 69 (100) [$C_5H_9^+$]; exact mass calculated for $C_{16}H_{18}Cl_2N_2OSe$ 403.9961; found 403.9948.

5-Chloro-6-methyl-3-phenyl-1-[5-(phenylselanyl)pentyl]-2(1*H*)-pyrazinone (20): This product was prepared by a general procedure described in ref.[10], starting from **19** (5.0 g). Yield: 4.0 g (72%); yellow crystals, m.p. 80−82 °C (Et_2O). IR (KBr, cm^{-1}): $\tilde{\nu}$ = 1649.5 (C=O), 1551.8 (C=N). ^1H NMR (300 MHz, $CDCl_3$): δ = 8.34−7.23 (m, 10 H, arom. H), 4.07 (m, 2 H, 1′-H), 2.92 (t, J = 7 Hz, 2 H, 5′-H), 2.15 (s, 3 H, CH_3), 1.80−1.58 (m, 4 H, 2′-H, 4′-H), 1.56 (m, 2 H, 3′-H) ppm. ^{13}C NMR (75 MHz, $CDCl_3$): δ = 154.9 (C-2), 148.3 (C-3), 135.1 (Se*C*-*ipso*), 134.2 (3-*C*-*ipso*), 132.6, 130.1, 130.0, 129.1, 128.9, 128.0, 126.8, 126.5 (C-*ortho*, C-*meta*, C-*para*, C-5, C-6), 46.2 (C-1′), 29.6 (C-2′), 27.44, 27.38, 27.0 (C-3′, C-4′, C-5′), 16.8 (CH_3) ppm. MS EI: *m*/*z* (%) = 446 (16) [$M^{\cdot+}$], 289 (100) [$M^{\cdot+}$ − SePh], 234 (18) [$M^{\cdot+}$ − C_4H_7SePh], 221 (31) [$M^{\cdot+}$ − C_5H_9SePh], 192 (31) [$M^{\cdot+}$ − $C_{12}H_{14}OSe$], 156 (13) [$PhSe^+$], 77 (18) [Ph^+], 69 (57) [$C_5H_9^+$]; exact mass calculated for $C_{22}H_{23}ClN_2OSe$ 446.0664; found 446.0655.

5-Chloro-6-methyl-1-(4-pentenyl)-3-phenyl-2(1*H*)-pyrazinone (21): *m*CPBA (70% with water, 0.4 g, 3 equiv.) in CH_2Cl_2 (20 mL) was added dropwise to a cooled (−15 °C) solution of **20** (500 mg, 11 mmol) in CH_2Cl_2 (50 mL). This mixture was warmed to room temp. and was then stirred for 30 min. After addition of DMS (98 µl, 2 equiv.) to work up the excess of reagent and DIPA (448 µl, 6 equiv.), elimination was effected by stirring at 60 °C overnight. After evaporation of the solvent, crude **21** was purified by column chromatography (silica gel, CH_2Cl_2). Yield: 297 mg (92%); yellow crystals, m.p.: 78−82 °C (Et_2O). IR (KBr, cm^{-1}): $\tilde{\nu}$ = 1644.9 (C=O), 1545.9 (C=N). ^1H NMR (300 MHz, $CDCl_3$): δ = 8.34 (m, 2 H, *ortho*-H), 7.43−7.40 (m, 3 H, *meta*-H, *para*-H), 5.84 (ddt, J = 18, 10, 7 Hz, 1 H, 4′-H), 5.15 (m, 2 H, 5′-H), 4.09 (m, 2 H, 1′-H), 2.52 (s, 3 H, 6-CH3), 2.21 (quart, J = 7 Hz, 2 H, 3′-H), 1.82 (quint, J = 7 Hz, 2 H, 2′-H) ppm. ^{13}C NMR (75 MHz, $CDCl_3$): δ = 155.0 (C-2), 148.2 (C-3), 136.6 (C-4′), 135.1 (C-5), 134.2 (C-*ipso*), 130.0, 128.9, 128.0 (C-*ortho*, C-*meta*, C-*para*), 126.5 (C-6), 116.1 (C-5′), 45.9 (C-1′), 31.0 (C-3′), 26.8 (C-2′), 16.7 (6-CH_3) ppm. MS EI: *m*/*z* (%) = 288 (75) [$M^{\cdot+}$], 273 (100) [$M^{\cdot+}$ − CH_3], 234 (54) [$M^{\cdot+}$ − C_4H_6], 220 (70) [$M^{\cdot+}$ − C_5H_8], 205 (32) [$M^{\cdot+}$ − C_4H_6 − CHO], 192 (27) [$M^{\cdot+}$ − C_5H_8 − CO]; exact mass calculated for $C_{16}H_{17}ClN_2O$ 288.1029; found 288.1034.

8-Methyl-1-phenyl-3,10-diazatricyclo[5.3.1.0^{3,8}]undecane-2,9-dione (23): The same procedure as employed for the preparation of compound **9** was used, starting from **21** (200 mg). Reaction time: 7 d. Yield: 146 mg (78%); white crystals, m.p. 243−244 °C (EtOAc). IR (KBr, cm^{-1}): $\tilde{\nu}$ = 3164.4 (NH), 1695.4 (C=O), 1686.0 (C=O). ^1H NMR (400 MHz, $CDCl_3$): δ = 7.45−7.39 (m, 5 H, arom. H), 6.48 (s, 1 H, 10-H), 4.00 (dd, J = 14, 6 Hz, 1 H, 4-H_{eq}), 3.25 (td, J = 13, 4 Hz, 1 H, 4-H_{ax}), 2.61 (dd, J = 13, 10 Hz, 1 H, 11′-H), 2.30 (m, 1 H, 7′-H), 2.19 (m, 1 H, 6-H_{ax}), 2.08 (dd, J = 13, 2.5 Hz, 1 H, 11-H), 1.80 (m, 1 H, 5-H_{ax}), 1.70 (s, 3 H, 8-CH_3), 1.58 (m, 1 H, 6-H_{eq}), 1.35 (m, 1 H, 5-H_{eq}) ppm. ^{13}C NMR (100 MHz, $CDCl_3$): δ = 179.0 (C-2), 171.2 (C-9), 135.3 (C-*ipso*), 128.9, 128.8, 127.3 (C-*ortho*, C-*meta*, C-*para*), 63.6, 63.1 (C-1, C-8), 42.8 (C-4), 37.2 (C-11), 36.0 (C-7), 23.9 (C-6), 16.3 (C-5), 15.6 (CH_3) ppm. MS EI: *m*/*z* (%) = 270 (32) [$M^{\cdot+}$], 186 (100) [$M^{\cdot+}$ − $(CH_2)_3NCO$], 158 (15) [$M^{\cdot+}$ − $(CH_2)_3NCO$ − CO]; exact mass calculated for $C_{16}H_{18}N_2O_2$ 270.1368; found 270.1371. Separation of the Enantiomers: The separation was achieved on a "Diacel OJ" column with chiral stationary phase, with a solvent gradient: 50% hexane/50% ethanol to 20% hexane/80% ethanol during 20 min. Flow: 1 mL/min.

***N*,8a-Dimethyl-8-oxo-6-phenyldecahydro[1,7]naphthyridine-6-carboxamide (24):** The same procedure as employed for the preparation of compound **10** was used, starting from **23** (100 mg). Yield: 111 mg (99%); slightly yellow crystals, m.p. 173−176 °C (CH_2Cl_2). IR (KBR, cm^{-1}): nu(tilde) = 1737.8 (C=O ester), 1656.0 (C=O lactam). ^1H NMR (400 MHz, $CDCl_3$): δ = 7.43−7.29 (m, 5 H, arom. H), 6.46 (s, 1 H, 7-H), 3.76 (s, 3 H, OCH_3), 3.01 (ddd, J = 14.5, 5.5, 1 Hz, 1 H, 5-H_{eq}), 2.86 (m (ddt), 1 H, 2-H_{eq}), 2.68 (ddd, J = 13, 10, 3 Hz, 1 H, 2-H_{ax}), 2.26 (dd, J = 14.5, 4 Hz, 1 H, 5-H_{ax}), 2.20 (br. s, 1 H, 1-H), 1.78−1.69 (m, 2 H, 4-H_{eq}, 4a-H), 1.63 (m, 1 H, 3-H_{eq}), 1.51 [m (qt), 1 H, 3-H_{ax}], 1.31 (s, 3 H, 8a-CH_3), 1.15 [m (qd), 1 H, 4-H_{ax}] ppm. ^{13}C NMR (75 MHz, $CDCl_3$): δ = 175.7 (CO_2CH_3), 172.1 (C-8), 142.1 (C-*ipso*), 129.1, 128.2, 124.0 (C-*ortho*, C-*meta*, C-*para*), 64.4 (C-6), 56.9 (C-8[a]), 53.3 (OCH_3), 42.7 (C-2), 37.7 (C-4a), 35.5 (C-5), 27.6 (C-4), 26.1 (8a-CH_3), 24.3 (C-3) ppm. Ms EI: *m*/*z* (%) = 302 (2) [$M^{\cdot+}$], 287 (10) [$M^{\cdot+}$ − CH_3], 259 (9) [$M^{\cdot+}$ − C_2H_5N], 110 (100) [$C_7H_{12}N^+$], 97 (39) [$C_6H_{11}N^+$]; exact mass calculated for $C_{17}H_{22}N_2O_3$ 302.1630; found 302.1634.

1-Acetyl-*N*,8a-dimethyl-8-oxo-6-phenyldecahydro[1,7]naphthyridine-6-carboxamide (25): The same procedure as employed for the preparation of compound **11** was used, starting from **24** (100 mg). Yield: 114 mg (100%); white crystals, m.p. 267−269 °C (Et_2O). IR (KBr, cm^{-1}): $\tilde{\nu}$ = 1665.9 (C=O), 1546.3 (C=O). ^1H NMR (400 MHz, [D_6]DMSO, 295 K): δ = 7.85 (s, 1 H, 7-H), 7.82 (br. q, J = 4 Hz, 1 H, N*H*Me), 7.45 (d, J = 8 Hz, 2 H, *ortho*-H), 7.35 (t, J = 7 Hz, 2 H, *meta*-H), 7.25 (t, J = 7 Hz, 1 H, *para*-H), 3.60 (br. d, J = 14 Hz, 1 H, 2-H_{eq}), 3.24 (ddd, J = 14, 11, 4 Hz, 1 H, 2-H_{ax}), 2.61 (d, J = 5 Hz, 3 H, NHCH_3), 2.41 (t, J = 14 Hz, 1 H, 5-H_{ax}), 2.05 (s, 3 H, COCH_3), 1.98 (br. d, J = 14 Hz, 1 H, 5-H_{eq}), 1.88 (tt, J = 14, 5 Hz, 1 H, 4-H_{ax}), 1.60−1.35 (m, 3 H, 4a-H, 3-H), 1.40 (s, 3 H, 8a-CH_3), 1.31 (br. d, J = 14 Hz, 1 H, 4-H_{eq}) ppm. ^{13}C NMR: δ = 172.8, 171.1, 169.5 (C=O), 142.7 (C-*ipso*), 127.8, 127.0 (C-*meta*, C-*para*), 126.1 (C-*ortho*), 63.9 (C-6), 58.4 (C-8a), 42.3 (C-2), 34.0 (C-4a), 33.8 (C-5), 26.1 (NH*C*H_3), 25.1 (C-4), 23.2 (CO*C*H_3), 22.7 (8a-*C*H_3), 21.8 (C-3) ppm. MS EI: *m*/*z* (%) = 343 (0.4) [$M^{\cdot+}$], 285 (100) [$M^{\cdot+}$ − $CONHCH_3$], 243 (79) [$M^{\cdot+}$ − CH_2O − $CONHCH_3$], 215 (16) [$C_{14}H_{19}N_2^+$], 198 (20) [$C_{14}H_{16}N^+$], 186 (27) [$C_{12}H_{12}NO^+$]; exact mass calculated for $C_{19}H_{25}N_3O_3$ 343.1896; found 343.1902.

Acknowledgments

The authors thank the FWO (Fund for Scientific Research − Flanders, Belgium) and the IUAP-4-11 funding by DWTC. We are grateful to R. De Boer for HRMS measurements, and to Prof. Piet Herdewyn of the Division of Medicinal Chemistry for providing Macromodel 5.0 and AMBER 6.0 for the MC and MD calculations. F. R. thanks the K. U. Leuven and W. D. B. [Postdoctoral Fellow of the Fund for Scientific Research Flanders (Belgium) FWO − Vlaanderen] thanks the FWO for the fellowships received.

[1] K.-C. Chou, *Anal. Biochem.* **2000**, *286*, 1−16 and references cited herein.

[2] For leading reviews on β-turn mimics and peptidomimetics see: [2a] V. J. Hruby, P. M. Balse, *Curr. Med. Chem.* **2000**, *7*,

945−970. [2b] R. M. J. Liskamp, *Recl. Trav. Chim. Pays-Bas* **1994**, *113*, 1−19. [2c] J. B. Ball, P. F. Alewood, *J. Mol. Recognit.* **1990**, *3*, 55−64. [2d] S. Hanessian, G. McNaughton-Smith, H.-G. Lombart, W. D. Lubell, *Tetrahedron* **1997**, *53*, 12789−12854.

[3] For some leading references on the incorporation of β-turn mimics see: [3a] R. M. Freidinger, D. F. Veber, D. S. Perlow, J. R. Brooks, R. Saperstein, *Science* **1980**, *210*, 656−658. [3b] M. G. Hinds, N. G. J. Richards, J. A. Robinson, *J. Chem. Soc., Chem. Commun.* **1988**, *22*, 1447−1449. [3c] M. Kahn, *Synlett* **1993**, *3*, 821−826. [3d] D. Gramberg, C. Weber, R. Beeli, J. Inglis, C. Burns, J. A. Robinson, *Helv. Chim. Acta* **1995**, *78*, 1588−1606. [3e] A. A. Virgilio, A. A. Bray, W. Zhang, L. Trinh, M. Snyder, M. M. Morrissey, J. A. Ellman, *Tetrahedron* **1997**, *53*, 6635−6644.

[4] W. M. De Borggraeve, F. R. Rombouts, E. V. Van der Eycken, S. M. Toppet, G. J. Hoornaert, *Tetrahedron Lett.* **2001**, *42*, 5693−5695.

[5] Recent examples are: [5a] Tuftsin: C. V. Valdeavella, H. D. Blatt, B. M. Pettitt, *Int. J. Pept. Protein Res.* **1995**, *46*, 372−380. [5b] Decorin/DS-PGII: Y. J. Wang, P. G. Scott, J. Sejbal, G. Kotovych, *Can. J. Chem.* **1996**, *74*, 389−401. [5c] Somatostatin: D. Gramberg, C. Weber, R. Beeli, J. Inglis, C. Bruns, J. A. Robinson, *Helv. Chim. Acta* **1995**, *78*, 1588−1606.

[6] A. Jabs, M. S. Weiss, R. Hilgenfeld, *J. Mol. Biol.* **1999**, *286*, 291−304.

[7] [7a] D. S. Kemp, E. T. Sun, *Tetrahedron Lett.* **1982**, *37*, 3759−3760. [7b] J.-P. Dumas, J. P. Germanas, *Tetrahedron Lett.* **1994**, *35*, 1493−1496. [7c] J. A. Robinson, D. Gramberg, *Tetrahedron Lett.* **1994**, *6*, 861−864. [7d] K. Kyonghee, J. P. Germanas, *J. Org. Chem.* **1997**, *62*, 2847−2852. [7e] P. K. C. Paul, P. A. Burney, M. M. Campbell, D. J. Osguthorpe, *Bioorg. Med. Chem. Lett.* **1992**, *2*, 141−144. [7f] L. Halab, W. D. Lubell, *J. Am. Chem. Soc.* **1999**, *64*, 3312−3321. [7g] S. Derrer, J. E. Davies, A. B. Holmes, *J. Chem. Soc., Perkin Trans. 1* **2000**, 2957−2967.

[8] F. J. R. Rombouts, W. De Borggraeve, S. M. Toppet, F. Compernolle, G. J. Hoornaert, *Tetrahedron Lett.* **2001**, *42*, 7397−7399.

[9] J. Vekemans, C. Pollers-Wieërs, G. Hoornaert, *J. Heterocycl. Chem.* **1983**, *20*, 919−923.

[10] K. J. Buysens, D. M. Vandenberghe, G. J. Hoornaert, *Tetrahedron* **1996**, *52*, 9161−9178.

[11] This method is misleadingly called a Monte Carlo conformer search. Monte Carlo simulations also generate structures by random displacements, but do not minimize the resulting structures. Instead, energies are calculated immediately and are used to obtain thermodynamic properties.

[12] Feature implemented in Macromodel, based on: C. A. G Haasnoot, F. A. A. M. de Leeuw, C. Altona, *Tetrahedron* **1980**, *36*, 2783−2792.

[13] Except for **26**, which can be viewed as a bridged Gly−Gly dipeptide, the bridged *cis*-amide mimics **1**, **2** and **27** shown in Figure 5 are the enantiomeric forms corresponding to the natural L-amino acids after omission of the bridging elements.

[14] J. B. Ball, P. F. Alewood, *J. Mol. Recognit.* **1990**, *3*, 55−64.

[15] J. B. Ball, R. A. Hughes, P. F. Alewood, P. R. Andrews, *Tetrahedron* **1993**, *49*, 3467−3478.

[16] G. Müller, G. Hessler, H. Y. Decornez, *Angew. Chem. Int. Ed.* **2000**, *39*, 894−896.

[17] P. N. Lewis, F. A. Momany, H. A. Scheraga, *Biochim. Biophys. Acta* **1973**, *303*, 211−229.

[18] F. J. R. Rombouts, D. A. J. Vanraes, J. Wynendaele, P. K. Loosen, I. Luyten, S. Toppet, F. Compernolle, G. J. Hoornaert, *Tetrahedron* **2001**, *57*, 3209−3220.

[19] F. Mohamadi, N. G. J. Richards, W. C. Guida, R. Liskamp, M. Lipton, C. Caufield, G. Chang, T. Hendrickson, W. C. Still, *J. Comput. Chem.* **1990**, *11*, 440−467.

[20] [20a] S. J. Weiner, P. A. Kollman, D. A. Case, U. C. Singh, C. Ghio, G. Algona, S. Profeta, Jr., P. J. Weiner, *J. Am. Chem. Soc.* **1984**, *106*, 765−784. [20b] S. J. Weiner, P. A. Kollman, D. T. Nguyen, D. A. Case, *J. Comput. Chem.* **1986**, *7*, 230−252.

[21] W. C. Still, A. Tempczyk, R. C. Hawley, T. Hendrickson, *J. Am. Chem. Soc.* **1990**, *112*, 6127−6129.

[22] [22a] G. Chang, W. C. Guida, W. C. Still, *J. Am. Chem. Soc.* **1989**, *111*, 4379−4386. [22b] M. Saunders, K. N. Houk, Y.-D. Wu, W. C. Still, M. Lipton, G. Chang, W. C. Guida, *J. Am. Chem. Soc.* **1990**, *112*, 1419−1427.

[23] S. Miertus, E. Scrocco, J. Tomasi, *J. Chem. Phys.* **1981**, *55*, 117−129.

[24] A. Klamt, G. Schuurmann, *J. Chem. Soc., Perkin Trans. 2* **1993**, 799−805.

[25] A. Klamt, *J. Phys. Chem.* **1995**, *99*, 2224−2235.

[26] A. Klamt, V. Jonas, T. Bürger, J. C. W. Lohrenz, *J. Phys. Chem. A* **1998**, *102*, 5074−5085.

[27] M. J. Frisch, G. W. Trucks, H. B. Schlegel, G. E. Scuseria, M. A. Robb, J. R. Cheeseman, V. G. Zakrzewski, J. A. Montgomery, R. E. Stratmann, J. C. Burant, S. Dapprich, J. M. Milliam, A. D. Daniels, K. N. Kudin, M. C. Strain, O. Farkas, J. Tomasi, V. Barone, M. Cossi, R. Cammi, B. Mennucci, C. Pomelli, C. Adamo, S. Clifford, J. Ochterski, G. A. Petersson, P. Y. Ayala, Q. Cui, K. Morokuma, D. K. Malick, A. D. Rabuck, K. Raghavachari, J. B. Foresman, J. Cioslowski, J. V. Ortiz, B. B. Stefanov, G. Liu, A. Liashenko, P. Piskorz, I. Komaromi, R. Gomperts, R. L. Martin, D. J. Fox, T. Keith, M. A. Al-Laham, C. Y. Peng, A. Nanayakkara, C. Gonzalez, M. Challacombe, P. M. W. Gill, B. G. Johnson, W. Chen, M. W. Wong, J. L. Andres, M. Head-Gordon, E. S. Replogle, J. A. Pople, *Gaussian 98 (Revision A.5)*, Gaussian Inc., Pittsburgh, PA, **1998**.

[28] W. D. Cornell, P. Cieplak, C. I. Bayly, I. R. Gould, K. M. Merz, Jr., D. M. Ferguson, D. C. Spellmeyer, T. Fox, J. W. Caldwell, P. A. Kollman, *J. Am. Chem. Soc.* **1995**, *117*, 5179−5197.

[29] W. L. Jorgensen, J. Chandrasekhar, J. D. Madura, R. W. Impey, M. L. Klein, *J. Chem. Phys.* **1983**, *79*, 926−935.

[30] ^{1}H and ^{13}C NMR spectra were taken at 50 °C, after addition of a drop of DCl.

[31] Resolution-enhancing Lorentz−Gauss function applied to FID: lb: −2.0 Hz; gb: 0.5 Hz.

[32] W. R. Bowman, P. T. Stephenson, N. K. Terret, A. R. Young, *Tetrahedron* **1995**, *51*, 7959−7980.

[33] T. Inaba, M. Fujita, K. Ogura, *J. Org. Chem.* **1991**, *56*, 1274−1279.

Received November 24, 2002

